



Double-ridge arrays metasurface for multifunctional splitter at terahertz

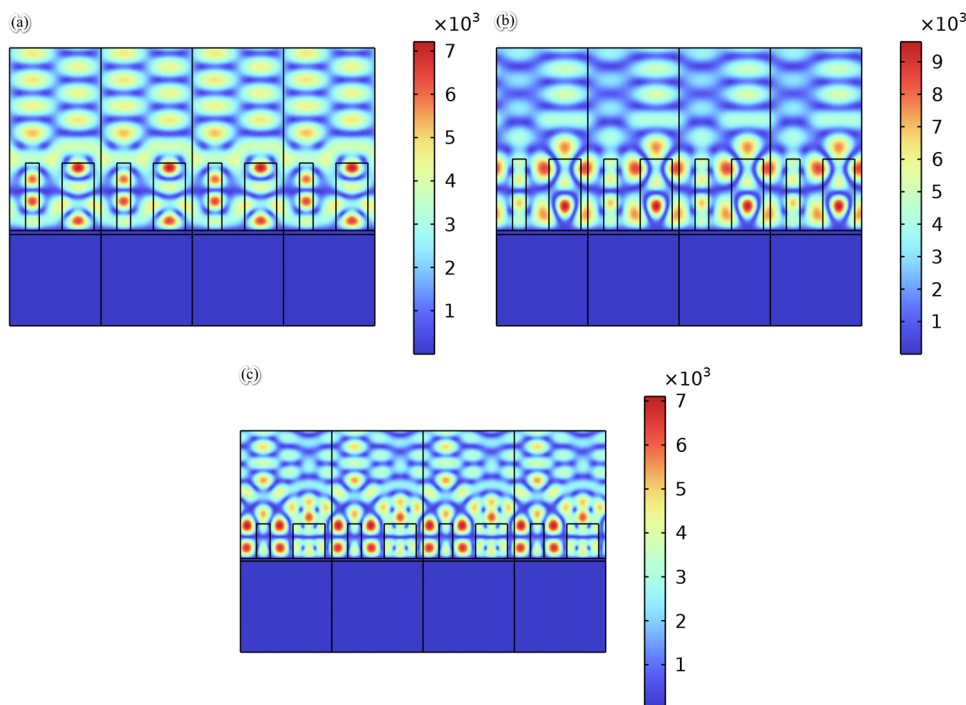
Liqun Liu¹ · Bo Wang¹ · Zherui Cui¹ · Hongwei Zhan¹ · Jinjie Li¹

Received: 4 October 2023 / Accepted: 21 December 2023 / Published online: 2 February 2024
© The Author(s), under exclusive licence to Springer-Verlag GmbH Germany, part of Springer Nature 2024

Abstract

In this paper, unlike many researches that focus on beam splitters based on gratings with symmetrical structures, an asymmetric grating with double-groove structure is proposed. Based on the double-groove grating, multi-port beam splitters including dual-port, three-port, and four-port, under normal incidence working at terahertz frequency are designed for both transverse-electric and transverse-magnetic polarizations. Rigorous couple-wave analysis and simulated annealing algorithm are employed to get the optimal parameters of the grating and accelerate the computing process. For the purpose of understanding the phenomenon of the beam incident, the finite element method is also applied to get the simulation result. It is proven that the proposed beam splitters all present great efficiency and uniformity on the energy distribution. High manufacturing tolerance of the beam splitters is also analyzed, which allows for greater flexibility in the fabrication process. Compared with beam splitters based on single-groove grating, multi-port beam splitters based on double grooves show great performance and universality.

Graphical abstract



1 Introduction

Optical grating metamaterials have been proven to be an essential part of many fields of science and technology. From spectroscopy and metrology [1] to telecommunications [2, 3] and biomedicine, these gratings offer unique and precise capabilities for manipulating and analyzing light in a variety of applications [4–6]. At their core, optical gratings consist of a periodic structure that modulates the refractive index of a material on a scale that is comparable to the wavelength of the light being diffracted. This modulation produces diffraction patterns that can be used for spectral analysis [7, 8], beam steering [9], optical sensing [10], and many other functions [11]. Meta-gratings achieve control over light by precisely arranging and designing micro- and nanostructures on a planar surface. These structures can be made of metals, dielectrics, or two-dimension materials, and their size and shape can be accurately manipulated to modulate the properties of incident light, such as refraction, reflection, and transmission. Reference [12] proposed a dynamic beam splitter incorporating all-dielectric metasurface in an elastic substrate. The optical behavior at a wavelength of 720 nm indicates that it not only exhibits pure optical diode behavior, but also functions as a dynamic beam splitter, with external mechanical stimulus of stretching. Although the structure is designed with wavelength at 720 nm, the design approach with appropriate materials can be used at any wavelength, including micro wave. Wan et. al. proposed a novel meta-grating design, which hybridizes the metasurface interfacial gradient with the blazed grating profile [13]. References [14] proposed a nanolithography technique to excite surface plasmon polariton (SPP) resonance to achieve nanomanufacturing beyond diffraction limits. This near-field exposure method can achieve high resolution and accuracy in nanomanufacturing.

The beam splitter is a very important type of optical grating, which has the ability to couple incident light into one or multiple diffraction orders [15]. It is understood that many studies have proposed high-performance single-groove beam splitters, which have one groove in a period. Due to the simple and symmetric structure, single-groove beam splitters can usually achieve better beam splitting performance and better uniformity under different polarizations, and single-groove beam splitters are more studied than beam splitters with double grooves. Huang et al. introduced multiple even beam splitters in the terahertz region based on their proposed subwavelength binary periodic rectangular shape, which is a single-groove structure [16]. The proposed beam splitters all show great diffraction efficiency and uniformity under transverse-electric (TE) polarization. Specifically optimized for TE-polarized

light, Hsu et al. designed a double-groove blazed grating for a seven-port beam splitter, achieving high efficiency of 91.39% [17]. Guo et al. also presented a beam splitter of double-groove fused-silica grating with three channels, which demonstrated outstanding beam splitter ability for TE polarization [18]. Wen et al. are the first to examine more than three diffracted orders using the modal technique, achieving a seven-port beam splitter with just the TE mode solved [19].

Terahertz waves refer to electromagnetic waves that have frequencies in the terahertz range from 0.1 to 10 terahertz. The wide bandwidth of terahertz waves enables high-speed data transmission and communication [20–22], and they are known for their unique ability to penetrate various materials, which makes them an attractive tool for imaging, sensing, detection and diagnostics applications [23–25]. Lin et al. proposed polarization-dependent terahertz reflective beam splitters, which can split the light into dual to seven ports [26]. Huang et al. proposed a single-groove beam splitter model with multiple functions [27]. It can function as four different kinds of splitter devices under terahertz waves, all exhibiting great efficiency under transverse-electric (TE) and transverse-magnetic (TM) polarizations.

In this paper, a double-groove grating model is proposed to design multi-function beam splitters working at the frequency of 2.52 THz. A dual-port, three-port, and four-port beam splitters are presented based on the double-groove grating model, which not only can work under TE polarization like the studies with double-groove structures [17–19], but also can function efficiently under TM polarization. Using rigorous coupled-wave algorithm (RCWA) [28, 29] and simulated annealing (SA) algorithm [30], the beam splitters optimized with optimum structural parameters show superior performance and great uniformity. To verify the optimal parameters obtained, finite element method (FEM) is also used to acquire the best results, which show agreement with the ones obtained by RCWA combined with SA.

2 Features of the double-groove grating

Figure 1 displays the three-dimensional structure of the double-groove grating. Under normal incidence, a beam of light under TE or TM polarizations is incident. The structure of the grating mainly consists of three parts, which are the grating ridges, reflective layer and the grating substrate. Grating ridges and substrate are both made of fused silica, whose refractive index is $n_1 = 1.45$ and thickness is represented by h_1 . The reflective layer is made of silver with a refractive index of $n_m = 0.144 + 11.366i$ and thickness $h_m = 10 \mu\text{m}$. The period of the grating is defined as d . Different from the common single-groove symmetric grating, grating ridges of the proposed grating structure

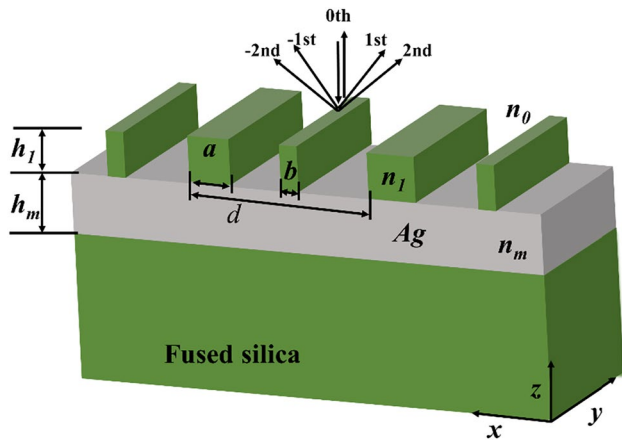


Fig. 1 Three-dimensional structure of the double-groove grating under normal incidence

are composed of two ridges, with width a and b respectively, in one period. As a result, there are two different duty cycle values defined in this grating, $f_1 = a/(2d)$ and

$f_2 = b/(2d)$, making this grating with a periodic but asymmetric structure. Between the ridges are full of air with refractive index $n_0 = 1.0$. The grating structure is designed for the application at the 2.52 THz, with the wavelength $\lambda = 118.83 \mu\text{m}$.

In terms of the proposed grating structure, the grating equation is written as:

$$\sin \theta_m - \sin \theta_{in} = \frac{m\lambda}{d}, \tag{1}$$

where θ_{in} is the incidence angle, which is 0 in this case, m signifies the m th diffraction order, θ_m represents the diffraction angle of m th order. To design reflective splitters with specific diffracted orders, the Eq. (1) can be turned into:

$$L\lambda < d < (L + 1)\lambda, \tag{2}$$

where $L = 1, 2, \dots, n$, and the beam splitters can be obtained with maximum $2L$ ports according to the equation. Therefore, under normal incidence, when period is designed between λ and 2λ , the double-groove grating structure can generate 2 or 3 diffraction orders, and four-port reflective

Table 1 Optimal parameters of two-port, three-port, and four-port beam splitters obtained by RCWA and SA

	TE polarization			TM polarization		
	Dual-port	Three-port	Four-port	Dual-port	Three-port	Four-port
λ (μm)	118.83			118.83		
f_1	0.3			0.3		
f_2	0.7			0.7		
d (μm)	222.00	224.00	353.66	222.00	224.00	344.30
h_1 (μm)	164.00	175.30	135.08	115.000	85.50	199.52

Table 2 Diffraction efficiency and uniformity of two-port, three-port, and four-port beam splitters obtained by RCWA and SA

	TE polarization (%)					TM polarization (%)				
	$\pm 2\text{nd}$	$\pm 1\text{st}$	0th	Total	U	$\pm 2\text{nd}$	$\pm 1\text{st}$	0th	Total	U
Dual-port	–	49.21	0.52	99.34	–	–	49.11	0.62	98.61	–
Three-port	–	33.12	33.16	99.29	0.22	–	33.17	33.16	99.38	0.17
Four-port	24.82	24.69	0.11	99.22	0.33	23.43	23.56	4.71	98.80	0.37

Table 3 Optimal parameters of two-port, three-port, and four-port beam splitters obtained by FEM, with wavelength $\lambda = 118.83 \mu\text{m}$, $f_1 = 0.3$, $f_2 = 0.7$

	TE polarization			TM polarization		
	Dual-port	Three-port	Four-port	Dual-port	Three-port	Four-port
d (μm)	223.5	223.89	353.70	217.10	230.80	343.20
h_1 (μm)	158.80	174.85	134.93	121.23	84.75	199.47

Table 4 Diffraction efficiency of two-port, three-port, and four-port beam splitters obtained by FEM with the parameters in Table 3

	TE polarization (%)				TM polarization (%)			
	$\pm 2\text{nd}$	$\pm 1\text{st}$	0th	Total	$\pm 2\text{nd}$	$\pm 1\text{st}$	0th	Total
Dual-port	–	48.33	2.1	99.28	–	48.29	2.5	99.13
Three-port	–	31.46	36.54	99.22	–	33.18	32.61	99.35
Four-port	25.31	24.17	0.14	99.23	20.50	26.96	4.18	99.12

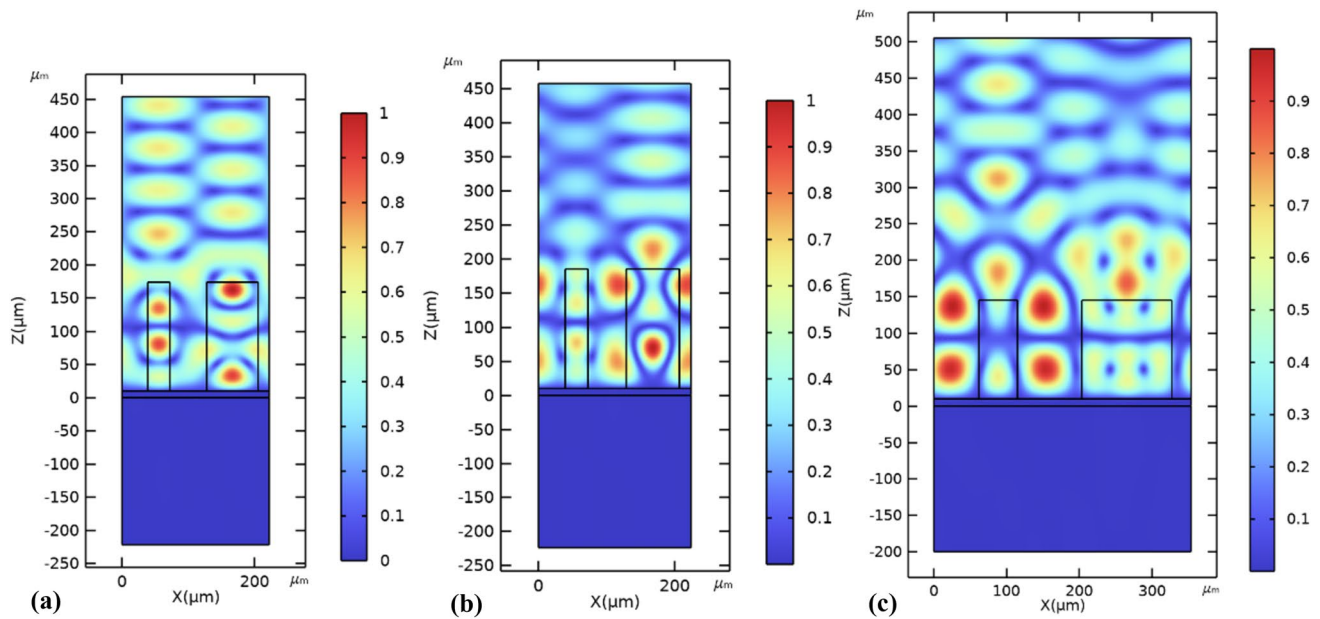


Fig. 2 Electric field distribution maps of the beam splitters for TE polarization under normal incidence with wavelength $\lambda = 118.83 \mu\text{m}$: **a** dual-port, **b** three-port, **c** four-port

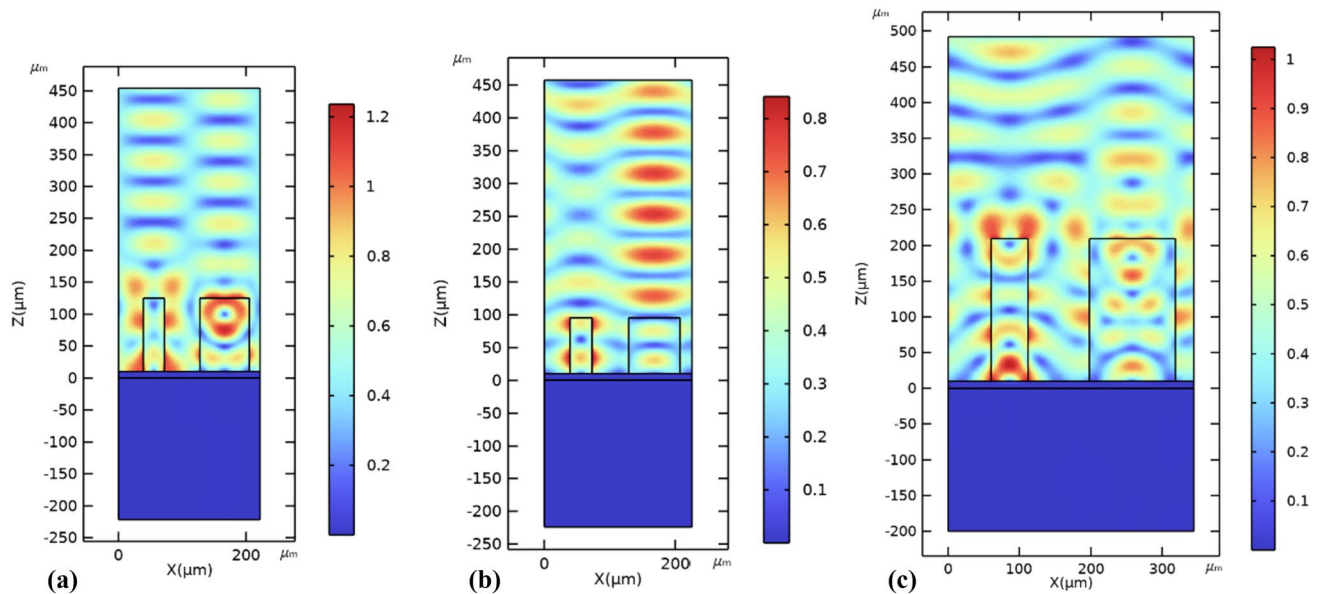


Fig. 3 Electric field distribution maps of the beam splitters for TM polarization under normal incidence with wavelength $\lambda = 118.83 \mu\text{m}$: **a** dual-port, **b** three-port, **c** four-port

beam splitter can also be designed when the period has a value between 2λ and 3λ .

There are four parameters to deal with base on the double-groove grating to realize reflective beam splitters, which are grating period d , grating depth h_1 , two duty cycle values f_1 and f_2 . Even if an asymmetric structure as the proposed grating containing two different ridges in one period, the double-groove grating has the periodic characteristics. RCWA is a

very effective method to solve the grating diffraction efficiency with the parameters of the grating structure. Hence, original parameters can be acquired using the RCWA.

RCWA is a very effective tool for dealing with electromagnetic field problems of periodic structures, especially diffraction gratings. This method involves expanding the electromagnetic field and the dielectric constant of the material into Fourier series, followed by solving eigenvalue

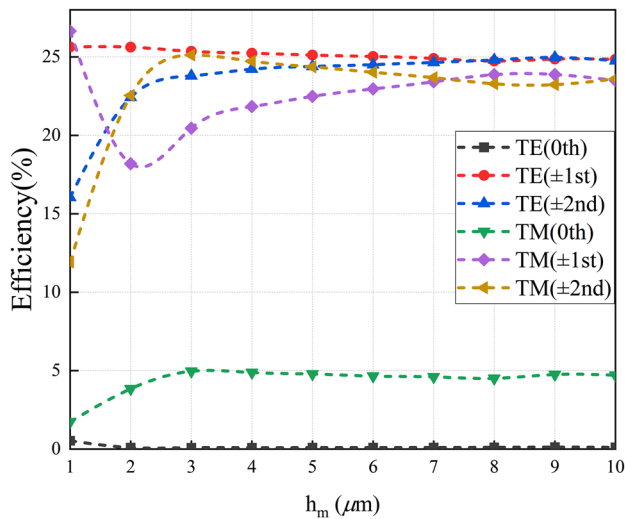


Fig. 4 Relationship between the thickness of the reflective layer h_m and diffraction efficiency

and eigenvector of the matrices to solve Maxwell's equations [28]. By using the eigenvalue method, the solutions to diffraction efficiency of each order are obtained (I_k of the objective functions are solved by RCWA, $k=0, \pm 1, \pm 2$). Subsequently, to use SA algorithm for optimization, objective functions for the beam splitters are required to be set. Based on the specified objective function, the SA algorithm randomly explores the whole solution space for its global optimal solution and finds the best optimization result. The objective functions for dual-port, three-port and four-port beam splitter are written as:

$$F_{\text{two}} = I_0, \tag{3}$$

$$F_{\text{three}} = \frac{\sum_{k=-1}^1 (I_k - I_v)^2}{\sum_{k=-1}^1 I_k}, \tag{4}$$

$$F_{\text{four}} = |I_0| + |I_1 - I_2|, \tag{5}$$

where I_k is the k th-order diffraction efficiency and I_v is the average diffraction efficiency of all the diffraction orders.

As mentioned above, RCWA can quickly calculate the diffraction efficiency of the k th order and along with SA algorithm the optimal parameters are computed. To achieve the polarization-independent feature, the grating needs to be optimized under both TE and TM polarizations. Hence, the ultimate objective function is:

$$F = \frac{F_{\text{TE}} + F_{\text{TM}}}{2}, \tag{6}$$

when the objective function hits the optimal value, a set of optimal parameters are obtained. Besides showing the performance of the beam splitters by the diffraction efficiency,

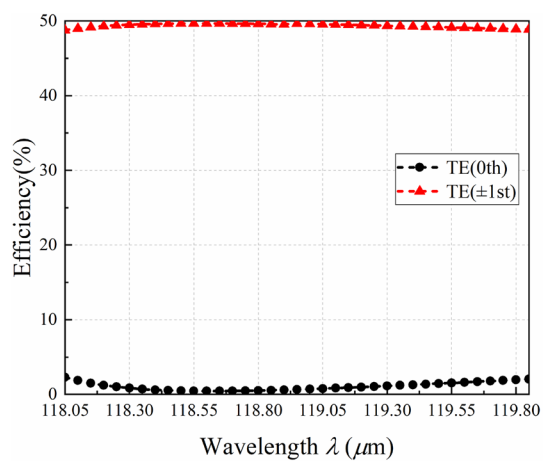
the uniformity of the beam splitters is also a parameter to measure the beam splitters' performance, which is defined as:

$$U = \frac{I_{\text{max}} - I_{\text{min}}}{I_{\text{max}} + I_{\text{min}}}. \tag{7}$$

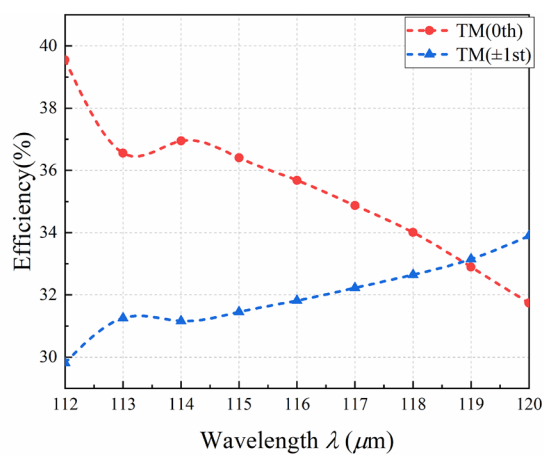
For a 2N-port beam splitter, I_{max} and I_{min} are the maximum and minimum diffraction efficiency of every order except the zeroth order, and for a 3-port beam splitter, they are the maximum and minimum diffraction efficiency of every diffraction order.

With the combination of RCWA and SA, three kinds of beam splitters are designed based on the double-groove gratin. There are two even beam splitters: a two-port beam splitter and four-port beam splitter with the feature of zeroth-order inhibition, and a three-port beam splitter. The beam splitters are designed with the conditions that working at a frequency of 2.52 THz, is normally incident by both TE-polarized and TM-polarized beams. The optimal parameters of the beam splitters are shown in Table 1. To simplify the calculation process, the values of f_1 and f_2 are fixed to 0.3 and 0.7 separately. Duty cycles, representing the widths of the grating ridges, are fixed in this case do not mean the widths of the grating ridges stay invariable. The procedure of determining the width of the grating ridges is being optimized concurrently with the search for the ideal value of the period. As a result, using the previously described method, the structural parameters of the grating have been properly optimized. Besides, based on the parameters obtained by RCWA and SA, the diffraction efficiency of every diffraction order of the designed beam splitters are displayed in Table 2. As the output of the beam splitters shows, the zeroth-order suppression for the dual-port and four-port beam splitters is well obtained with the double-groove structure. The uniformity and overall efficiency are superior and reliable with the output from different channels. To compare with the optimal parameters obtained above, as in Refs. [31, 32], FEM is used to optimize the structure of the grating. FEM is a numerical analysis technique used to solve physical problems in structures, fluid dynamics, heat transfer, electromagnetic fields, and other areas. It converts continuous physical problems into a discrete form by establishing a finite element model. The entire solution domain is divided into numerous small elements, and numerical methods are applied to analyze each individual element. Ultimately, an approximate solution for the entire system is obtained. Tables 3 and 4 display the results obtained by using FEM. Among the results, the dual-port beam splitter has a relatively large offset for the larger tolerance it exhibits. It is obvious that the optimization results obtained from both RCWA with SA and FEM are consistent.

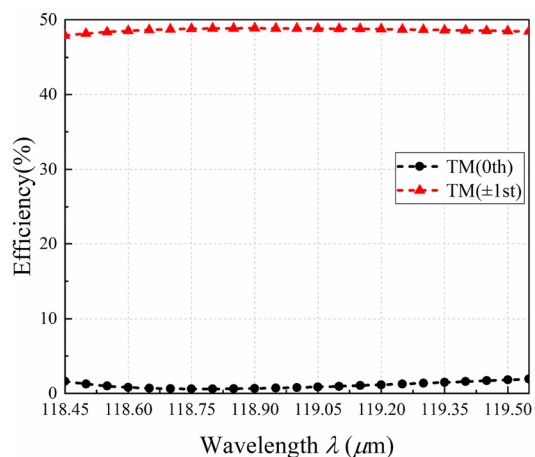
To visualize the reflective effect of the energy when beam is normally incident under both polarizations, the electric



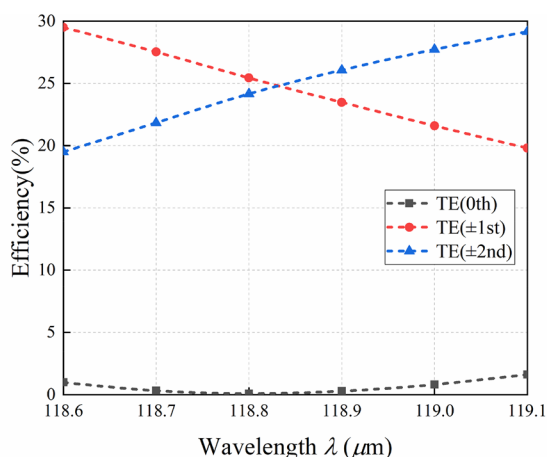
(a)



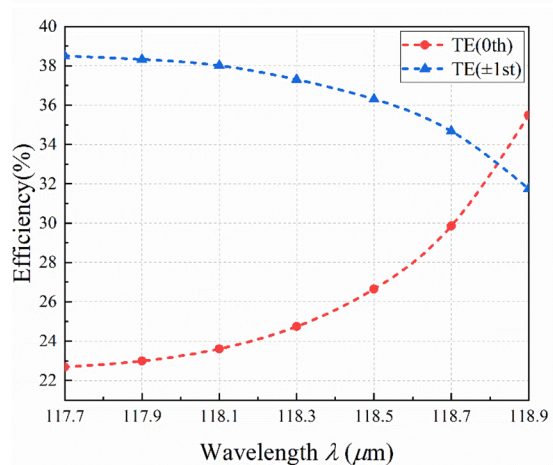
(d)



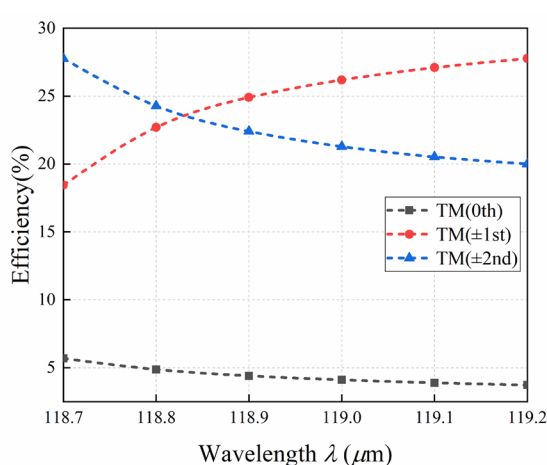
(b)



(e)



(c)



(f)

Fig. 5 Relationship of the beam splitters between diffraction efficiency and wavelength under TE and TM polarizations: **a** dual-port under TE polarization, **b** dual-port under TM polarization, **c** three-

port under TE polarization, **d** three-port under TM polarization, **e** four-port under TE polarization, **f** four-port under TM polarization

Table 5 Comparison of the tolerance for the proposed polarization-dependent terahertz reflective beam splitters and the beam splitters proposed in Ref. [26]

	Output modes	Efficiency	λ (μm)	d (μm)	h_1 (μm)
This paper	Dual-port	$\eta_{\text{TE}} > 45.00\%$	118.10–119.51	595.88–605.45	32.03–35.18
		$\eta_{\text{TM}} > 45.00\%$	118.45–120.21	590.18–605.75	19.874–23.70
	Three-port	$\eta_{\text{TE}} > 30.00\%$	118.73–118.87	599.78–600.51	376.58–379.44
		$\eta_{\text{TM}} > 30.00\%$	118.79–118.85	599.78–600.53	163.87–164.29
	Four-port	$\eta_{\text{TE}} > 22.00\%$	118.82–118.84	599.85–600.30	437.92–438.06
		$\eta_{\text{TM}} > 22.00\%$	118.82–118.88	599.61–600.91	593.75–594.04
	Dual-port	$\eta_{\text{TE}} > 45.50\%$	117.75–123.55	209.38–224.54	156.00–172.50
		$\eta_{\text{TM}} > 45.50\%$	118.20–122.60	206.08–223.39	109.65–117.80
	Three-port	$\eta_{\text{TE}} > 30.00\%$	118.72–118.98	223.70–224.20	173.94–177.20
		$\eta_{\text{TM}} > 30.00\%$	112.78–121.80	197.17–236.96	82.60–102.20
	Four-port	$\eta_{\text{TE}} > 22.00\%$	118.71–118.95	353.15–354.15	134.26–135.82
		$\eta_{\text{TM}} > 22.00\%$	118.78–118.93	344.00–344.60	198.98–199.86

field distribution maps of the beam splitters are shown in Figs. 2 and 3. It can be seen from the maps that the energy of the plane waves for both polarizations is basically reflected on the grating ridges and grating grooves when the light hits the grating. With the double-groove structure which is asymmetric, the grating can show descent periodic characteristics. As a result of the reflecting phenomena, nearly no energy is transmitted through the substrate surrounding the reflective layer, which is in line with the outcome of achieving high diffraction efficiency. This further establishes the reflective layer's reasonable design. To maximize the reflection efficiency and eliminate the transmission efficiency, the Ag layer is added, suppressing transmission phenomenon. Taking the four-port beam splitter as an example, the relationship between the thickness of reflective layer and diffraction efficiency is described in Fig. 4. The figure shows that the non-zero order diffraction efficiency steadily grows, while the zeroth-order efficiency remains at a very low efficiency value as the thickness of the reflective layer increases. For the reason of saving manufacturing cost, the thickness can be set at 7 μm . It is worth noting that the design does not work at transmissive state when the Ag reflector is removed.

3 Investigation and discussion

After the design and optimization processes are complete, beam splitters based on the double-groove grating structure need to be thoroughly analyzed [33, 34]. The symmetry rule predicts that the diffraction efficiency for each non-zero order will be the same on either side of the zeroth order, since the diffracted waves are symmetrically distributed with respect to the normal of the grating surface. Figure 5 illustrates the analytical findings for each beam splitter and the correlation between diffraction efficiency and wavelength. As you can see, diffraction efficiency of the beam splitters can be sufficiently and steadily maintained over a

large bandwidth for both TE and TM polarizations, especially for dual-port beam splitter with efficiencies of ± 1 orders exceeding 48% and falling below 5% at the 0th order. Table 5 shows the wavelength tolerance of the beam splitters. It is reasonable to assume that the wavelength tolerance will decrease as the number of output ports increases. Period is a significant parameter since the output ports of the grating are determined by its value when the working frequency is set at 2.52 THz. Figure 6 describes diffraction efficiency versus grating period of the beam splitters under both TE and TM polarizations. Similar to the wavelength, beam splitters with multiple ports are all showing superior and reliable performance on the period, while covering wide tolerance ranges. By comparison, the four-port beam splitter comes with a relatively narrow range as present in Table 5. The grating period tolerance does, however, not significantly affect the diffraction efficiency when employing the method described in Ref. [35] due to the great precision of the fabrication process.

One important parameter that affects the diffraction efficiency of a grating is the depth of the grooves. In general, deeper grooves result in higher diffraction efficiency. However, deep grooves can also lead to mechanical instability, fabrication difficulties, and increased sensitivity to environmental factors such as temperature and humidity. Figure 7 displays the influence on the diffraction efficiency made by the grating depth. While other parameters are set with ideal values, the grating depth of the double grooves exhibits great manufacturing tolerance.

Table 5 lists the manufacturing tolerance for the performance of the beam splitters with various ports under TE and TM polarizations. Additionally, a comparison between the beam splitters suggested in Ref. [26] and this research is investigated. The data demonstrates that the beam splitters developed in this work achieve higher tolerance. Comparison diffraction efficiency of the proposed beam splitters with 2-port beam splitter suggested in Ref. [36],

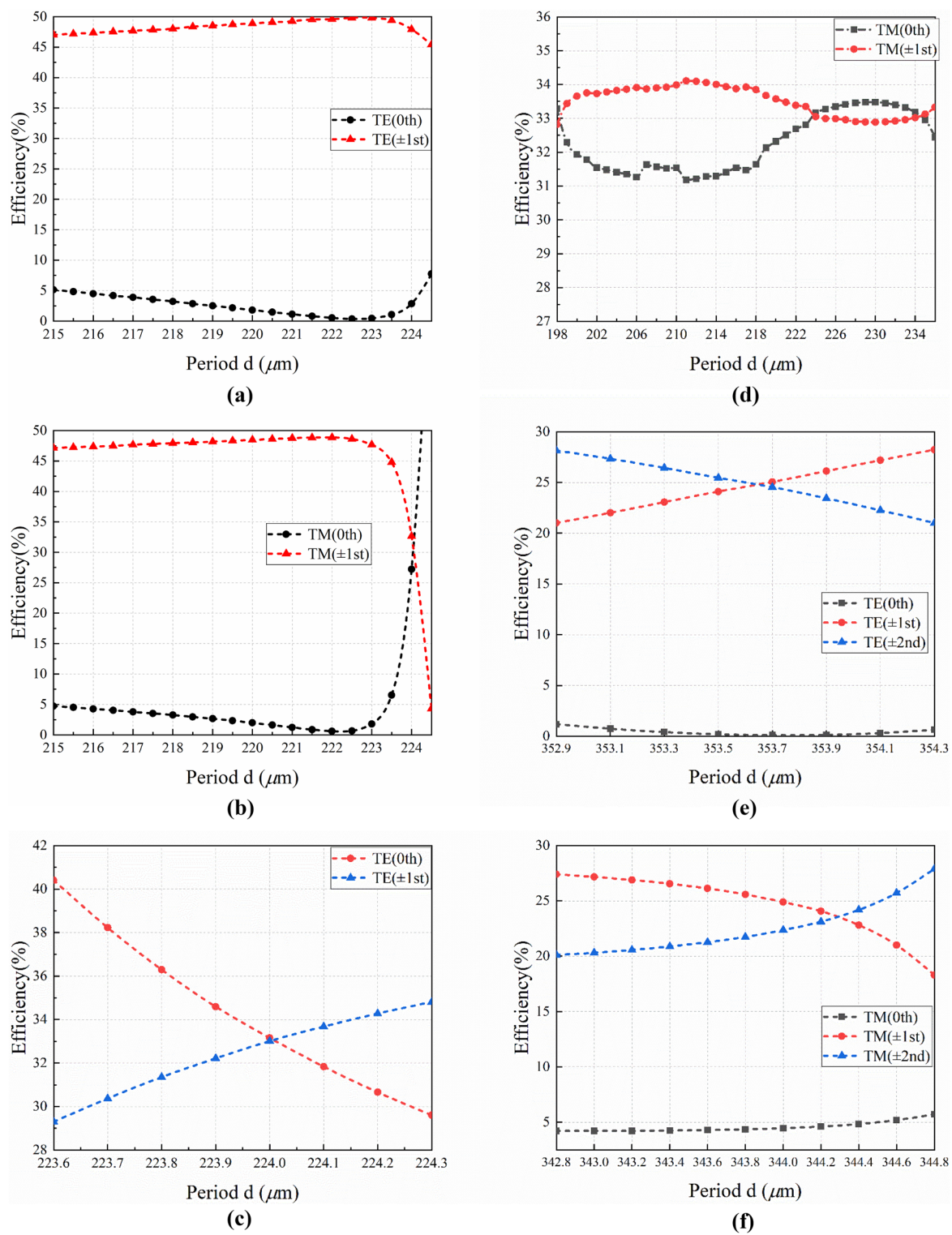


Fig. 6 Relationship of the beam splitters between diffraction efficiency and period under TE and TM polarizations: **a** dual-port under TE polarization, **b** dual-port under TM polarization, **c** three-port

under TE polarization, **d** three-port under TM polarization, **e** four-port under TE polarization, **f** four-port under TM polarization

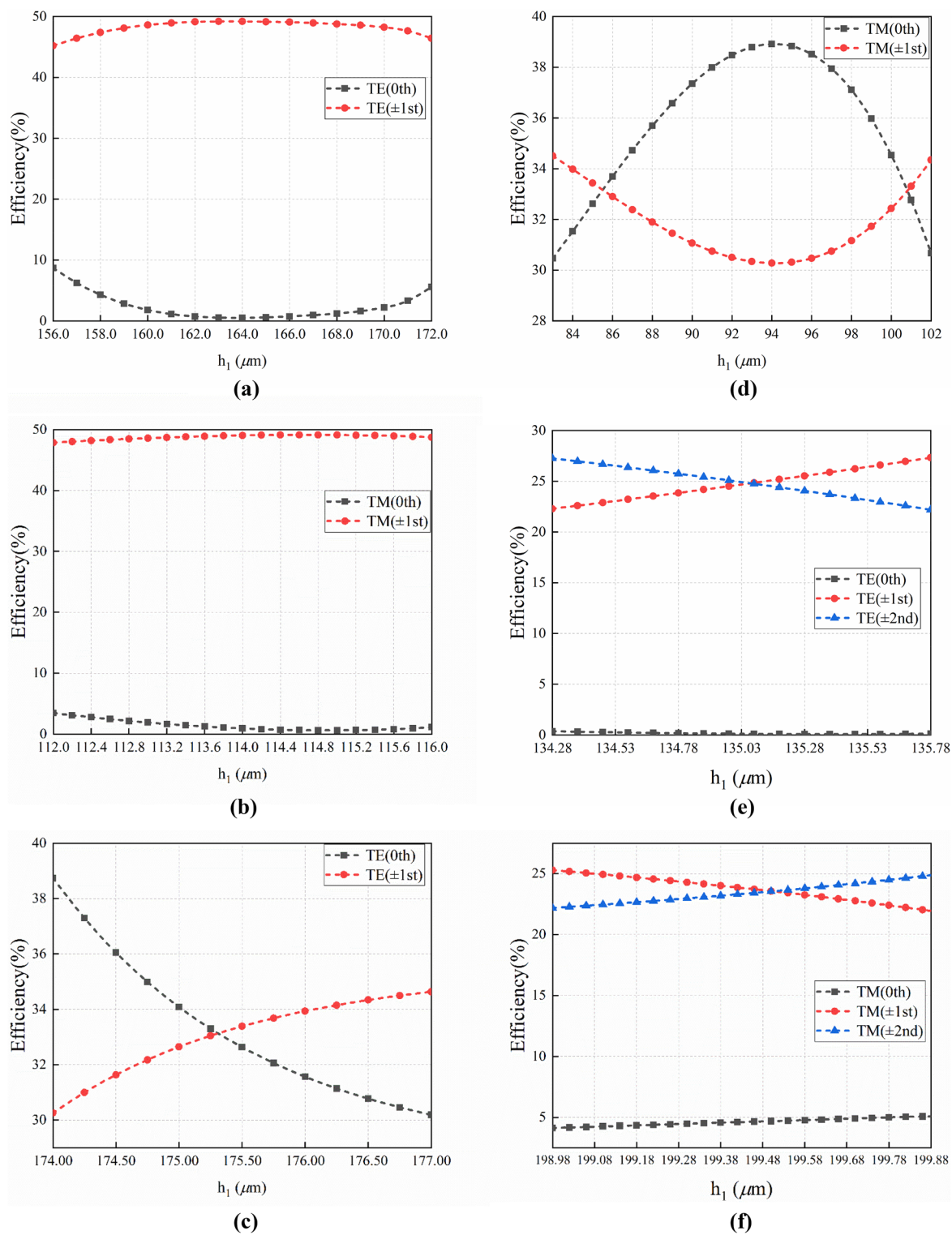


Fig. 7 Relationship of the beam splitters between grating depth h_1 and diffraction efficiency under TE and TM polarizations: **a** dual-port under TE polarization, **b** dual-port under TM polarization, **c** three-

port under TE polarization, **d** three-port under TM polarization, **e** four-port under TE polarization, **f** four-port under TM polarization

Table 6 Comparison of the diffraction efficiency of the beam splitters reported in other researches and this work

Port		Grooves	$\eta_{\pm 2}^{\text{TE}}$ (%)	$\eta_{\pm 1}^{\text{TE}}$ (%)	Total (%)	$\eta_{\pm 2}^{\text{TM}}$ (%)	$\eta_{\pm 1}^{\text{TM}}$ (%)	Total (%)
2	Ref. [36]	Single	–	46.54	93.08	–	47.74	95.48
	This work	Double	–	49.21	99.34	–	49.11	98.61
4	Ref. [37]	Single	23.29	24.29	–	23.01	23.03	–
	Ref. [38]	Single	23.61	23.47	94.16	23.79	23.45	94.48
	This work	double	24.82	24.69	99.22	23.43	23.56	98.80

4-port beam splitter in Refs. [37, 38] is listed in Table 6. The performance of the beam splitters obtained from the double-groove grating is better than those based on single-groove grating, and the double-groove grating has remarkable universality to create beam splitters with different output ports. The beam splitters based on the same structure in this paper exhibit better efficiency compared with other beam splitters proposed in different researches. It is thought that the grating structure and optimization techniques used in the article can streamline the production process and serve as an example for producing multi-port beam splitters, which would enable beam splitters to perform multiple functions.

The experimental manufacturing process of the multi-port beam splitter proposed in this article can refer to Refs. [39, 40]. As Ref. [39] mentions, the production of high-density gratings can be achieved through holographic interference recording and inductively coupled plasma (ICP) etching technology, which is particularly effective for the manufacturing of fused-silica gratings. They used the RCWA method to optimize a two-port beam splitter and fabricated with the aforementioned techniques. The experimental results obtained were in excellent agreement with the theoretical values. Reference [40] employed RCWA in the optimization of their beam splitter and utilized nanoimprint lithography (NIL) to produce metal wire grating structures on quartz substrates. As anticipated, their grating also achieved good broadband effects. Moreover, relevant experiments on the fabrication of the gratings are demonstrated in Refs. [41, 42], which verified the feasibility of the proposed beam splitters in actual manufacturing.

4 Conclusions

In this paper, a double-groove structure grating is proposed and beam splitters are designed based on it. The investigation of this asymmetric grating structure with double grooves represents a departure from traditional single-groove grating designs. Using RCWA and SA to design and optimize the structure, dual-port, three-port and four-port beam splitters working in terahertz region all present great efficiency and

stable uniformity. FEM is also employed to verify the optimal parameters and visualize the phenomenon of the reflection process. In addition to being built to create outstanding beam splitters for TE mode like earlier reported researches, the proposed grating can perform well as a multi-port beam splitter in TM mode. The study of the beam splitters' manufacturing tolerance on a double-groove basis shows excellent results. Overall, a grating that has high tolerance of groove depth is a valuable tool for many applications where stability and reliability are critical. It enables the grating to perform consistently over a wide range of conditions. This research offers promising avenues for further investigation.

Acknowledgements This work is supported by the Key Laboratory of Biomedical Imaging Science and System, Chinese Academy of Sciences.

Author contributions LL: Data curation, Formal analysis, Validation, Investigation, Writing—original draft. BW: Conceptualization, Methodology, Supervision, Project administration, Writing—review and editing. ZC: Formal analysis. HZ: Investigation. JL: Investigation.

Data availability The data analyzed during the current study are available from the corresponding author on reasonable request.

Declarations

Conflict of interest The authors declare no competing interests.

References

1. Y. Kayser, C. David, U. Flechsig, J. Krempasky, V. Schlott, R. Abela, X-ray grating interferometer for in situ and at-wavelength wavefront metrology. *J. Synchrotron Radiat.* **24**(1), 150–162 (2017)
2. L.R. Chen, J. Wang, B. Naghdi, I. Glesk, Subwavelength grating waveguide devices for telecommunications applications. *IEEE J. Sel. Top. Quantum Electron.* **25**(3), 1–11 (2019)
3. T. Loukina, S. Massenet, R. Chevallier, K. Heggarty, N.M. Shigapova, A. Skochilov, Volume diffraction gratings for optical telecommunications applications: design study for a spectral equalizer. *Opt. Eng.* **43**(11), 2658–2665 (2004)
4. G. Zhou, Z.H. Lim, Y. Qi, F.S. Chau, G. Zhou, Mems gratings and their applications. *Int. J. Optomechatron.* **15**(1), 61–86 (2021)

5. H. Tamiya, Y. Mitera, K. Taniguchi, H. Aoyama, K. Yamazaki, Development of a three-dimensional encoder for highly accurate positioning. *J. Jpn. Soc. Precis. Eng.* **85**(10), 891–895 (2019)
6. A. Othonos, K. Kalli, G.E. Kohnke, Fiber bragg gratings: fundamentals and applications in telecommunications and sensing. *Phys. Today* **53**(5), 61–62 (2000)
7. Y. Tachikawa, Spectral analysis of transmission echelon grating filters for photonic networks. *Opt. Rev.* **6**(2), 131–138 (1999)
8. E.S. Lee, J.Y. Lee, Symmetry exploitation of diffraction gratings to enhance the spectral resolution. *J. Opt. Soc. Korea* **15**(3), 216–221 (2011)
9. J. Kim, M.N. Miskiewicz, S. Serati, M.J. Escuti, Nonmechanical laser beam steering based on polymer polarization gratings: design optimization and demonstration. *J. Lightw. Technol.* **33**(10), 2068–2077 (2015)
10. F. Baldini, M. Brenci, F. Chiavaioli, A. Giannetti, C. Trono, Optical fibre gratings as tools for chemical and biochemical sensing. *Anal. Bioanal. Chem.* **402**(1), 109–116 (2012)
11. J. Marciante, N. Farmiga, J. Hirsh, M. Evans, H. Ta, Optical measurement of depth and duty cycle for binary diffraction gratings with subwavelength features. *Appl. Opt.* **42**, 3234–3240 (2003)
12. H. Kocer, Y. Durna, H. Kurt, E. Ozbay, Dynamic beam splitter employing an all-dielectric metasurface based on an elastic substrate. *Opt. Lett.* **45**(13), 3521–3524 (2020)
13. C. Wan, R. Yang, Y. Shi, G. Zheng, Z. Li, Visible-frequency meta-gratings for light steering, beam splitting and absorption tunable functionality. *Opt. Express* **27**(26), 37318–37326 (2019)
14. X. Luo, T. Ishihara, Surface plasmon resonant interference nanolithography technique. *Appl. Phys. Lett.* **84**(23), 4780–4782 (2004)
15. S. Yin, D. Zeng, Y. Chen, W. Huang, C. Zhang, W. Zhang, E. Yiwen, Optically controlled terahertz dynamic beam splitter with adjustable split ratio. *Nanomaterials (Basel)* **12**(7), 1169 (2022)
16. H. Huang, S. Ruan, T. Yang, P. Xu, Novel even beam splitters based on subwavelength binary simple periodic rectangular structure. *Nano-Micro Lett.* **7**(2), 177–182 (2015)
17. J. Hsu, C. Lee, R. Chen, A high-efficiency multi-beam splitter for optical pickups using ultra-precision manufacturing. *Microelectron. Eng.* **113**, 74–79 (2014)
18. L. Guo, J. Ma, Broad band beam splitter based on the double-groove fused silica grating. *Optik* **125**(1), 232–234 (2014)
19. F.J. Wen, P.S. Chung, Design of a high-efficiency seven-port beam splitter using a dual duty cycle grating structure. *Appl. Opt.* **50**(19), 3187–3190 (2011)
20. T. Nagatsuma, G. Ducournau, C.C. Renaud, Advances in terahertz communications accelerated by photonics. *Nat. Photon.* **10**(6), 371–379 (2016)
21. L. Tohmé, S. Blin, G. Ducournau, P. Nouvel, D. Coquillat, S. Hisatake, T. Nagatsuma, A. Pénarier, L. Varani, W. Knap, J.F. Lampin, Terahertz wireless communication using GaAs transistors as detectors. *Electron. Lett.* **50**(4), 323–325 (2014)
22. R.S. Nishtha, A.K. Yaduvanshi, A.K. Kushwaha, Pandit, Terahertz rectangular dra for high speed communication applications. *J. Discrete Math. Sci. Cryptogr.* **24**(5), 1205–1214 (2021)
23. V.Y. Fedorov, S. Tzortzakis, Powerful terahertz waves from long-wavelength infrared laser filaments. *Light Sci. Appl.* **9**(1), 186 (2020)
24. L. Wang, Terahertz imaging for breast cancer detection. *Sensors (Basel)* **21**(19), 6465 (2021)
25. X. Yang, X. Zhao, K. Yang, Y. Liu, Y. Liu, W. Fu, Y. Luo, Biomedical applications of terahertz spectroscopy and imaging. *Trends Biotechnol.* **34**(10), 810–824 (2016)
26. Z. Lin, B. Wang, X. Xing, F. Zhang, J. Xue, J. Zhou, Polarization-sensitive terahertz reflective multi-channel beam separation by cascaded configuration. *Results Phys.* **28**, 104702 (2021)
27. Z. Huang, B. Wang, Multi-function beam control of terahertz wave by hybrid metamaterial. *Laser Phys.* **31**(12), 126202 (2021)
28. M.G. Moharam, D.A. Pomet, E.B. Grann, T.K. Gaylord, Stable implementation of the rigorous coupled-wave analysis for surface-relief gratings: Enhanced transmittance matrix approach. *J. Opt. Soc. Am. A* **12**(5), 1077–1086 (1995)
29. J. Zheng, C. Zhou, B. Wang, F. Jijun, Beam splitting of low-contrast binary gratings under second Bragg angle incidence. *J. Opt. Soc. Am. A Opt. Image Sci. Vis.* **25**, 1075–1083 (2008)
30. W. Liu, G. Jin, Y. Xie, P. Sun, B. Zhou, W. Jia, J. Wang, C. Zhou, Broadband high-efficiency polarization-independent double-layer slanted grating for rgb colors. *Opt. Commun.* **488**, 126864 (2021)
31. Z. Huang, B. Wang, Z. Lin, K. Wen, Z. Meng, F. Zhang, Z. Nie, X. Xing, L. Chen, L. Lei, J. Zhou, Newly reflective bi-function beam splitter by SiO₂ pencil-like arrays on silver plate. *Optik* **242**, 167289 (2021)
32. H. Li, T. Huang, L. Lu, Z. Hu, B. Yu, High-efficiency nine-port beam splitting output enabled by a dielectric lamellar sandwiched fused-silica grating. *Opt. Laser Technol.* **145**, 10765 (2022)
33. P. Koleják, G. Lezier, K. Postava, J.-F. Lampin, N. Tiercelin, M. Vanwollegem, 360° polarization control of terahertz spintronic emitters using uniaxial feco/tbco2/feco trilayers. *ACS Photon.* **9**(4), 1274–1285 (2022)
34. J.A. Fülöp, S. Tzortzakis, T. Kampfrath, Laser-driven strong-field terahertz sources. *Adv. Opt. Mater.* **8**(3), 1900681 (2019)
35. Y. Xie, W. Jia, D. Zhao, Z. Ye, P. Sun, C. Xiang, J. Wang, C. Zhou, Traceable and long-range grating pitch measurement with picometer resolution. *Opt. Commun.* **476**, 126316 (2020)
36. Z. Xiong, B. Wang, J. Zhou, Triple-layer array splitter for zeroth-order suppressing under normal incidence. *Optik* **267**, 169743 (2022)
37. C. Fu, B. Wang, Z. Lin, Z. Huang, K. Wen, Z. Meng, Z. Nie, X. Xing, L. Chen, L. Lei, J. Zhou, Beam generator of 4-channel with zeroth order suppressed by reflective t-type grating. *Mod. Phys. Lett. B* **35**(13), 2150218 (2021)
38. C. Gao, B. Wang, Four equal-intensity laser output and physical analysis generated by reflective grating with a silver plate. *Laser Phys.* **30**(2), 026203 (2020)
39. J. Feng, C. Zhou, J. Zheng, H. Cao, P. Lv, Design and fabrication of a polarization-independent two-port beam splitter. *Appl. Opt.* **48**(29), 5636–5641 (2009)
40. L. Zhang, C. Li, J. Li, F. Zhang, L. Shi, Design and fabrication of metal-wire nanograting used as polarizing beam splitter in optical telecommunication. *Optoelectron. Adv. Mat.* **1**(6), 263–266 (2007)
41. S. Joseph, S. Sarkar, J. Joseph, Grating-coupled surface plasmon-polariton sensing at a flat metal-analyte interface in a hybrid-configuration. *ACS Appl. Mater. Int.* **12**(41), 46519–46529 (2020)
42. S. Sarkar, S. Poulouse, P.K. Sahoo, J. Joseph, Flexible and stretchable guided-mode resonant optical sensor: Single-step fabrication on a surface engineered polydimethylsiloxane substrate. *Osa Continuum.* **1**(4), 1277–1286 (2018)

Publisher's Note Springer Nature remains neutral with regard to jurisdictional claims in published maps and institutional affiliations.

Springer Nature or its licensor (e.g. a society or other partner) holds exclusive rights to this article under a publishing agreement with the author(s) or other rightsholder(s); author self-archiving of the accepted manuscript version of this article is solely governed by the terms of such publishing agreement and applicable law.

Authors and Affiliations

Liqun Liu¹ · Bo Wang¹ · Zherui Cui¹ · Hongwei Zhan¹ · Jinjie Li¹

✉ Bo Wang
wangb_wsx@yeah.net

¹ School of Physics and Optoelectronic Engineering,
Guangdong University of Technology, Guangzhou 510006,
China